Terr. Atmos. Ocean. Sci., Vol. 30, No. 5, 695-704, October 2019 doi: 10.3319/TAO.2019.01.10.02

Temperature as a tracer for fluid movement at hydrothermal sites near the Yonaguni Knoll IV, Okinawa Trough

Ting-Wei Wu[1, 2], Wu-Cheng Chi[1, *], Yu-Sian Lin[1], and Song-Chuen Chen[3]

[1] *Institute of Earth Sciences, Academia Sinica, Taipei City, Taiwan*
[2] *MARUM - Center for Marine Environmental Sciences, University of Bremen, Bremen, Germany*
[3] *Central Geological Survey, Ministry of Economic Affairs, Taipei City, Taiwan*

Article history:
Received 30 April 2018
Revised 26 November 2018
Accepted 10 January 2019

Keywords:
Hydrothermal Modeling, Fluid Flow Rate, Péclet Number, Yonaguni Knoll IV

Citation:
Wu, T.-W., W.-C. Chi, Y.-S. Lin, and S.-C. Chen, 2019: Temperature as a tracer for fluid movement at hydrothermal sites near the Yonaguni Knoll IV, Okinawa Trough. Terr. Atmos. Ocean. Sci., 30, 695-704, doi: 10.3319/TAO.2019.01.10.02

ABSTRACT

This paper aims to understand the hydrothermal sites near the Yonaguni Knoll IV in the Okinawa Trough, and to develop new techniques to study fluid flow patterns for hydrothermal systems and their impact on ore deposits on the seafloor. Hydraulic parameters are important for hydrothermal system studies, but *in-situ* measurements of fluid migration rates are difficult. Hydrothermal fluids can reach several hundred degrees Celsius, temperatures high enough to perturb hydrothermal fields and pore water migration patterns. Using *in-situ* temperature data as constraints, we model and synthesize 1-D and 3-D cylindrical hydrothermal models to fit the spatial variations of observed temperature fields. The 1-D modeling uses Péclet number analysis along the conduit. We also construct a 3-D cylindrical model to estimate the temperature and fluid velocity fields using a finite element software. All domains are set to be porous to allow the fluid to flow. The simulation is run until it reaches a semi steady-state solution, allowing both the temperature and velocity fields to stabilize. Results show the dimension of the thermal anomaly zone is likely controlled by advective heat transfer along the vent due to upward fluid flow. We estimate a Péclet number of -1.6, and the vertical fluid flow velocities at these sites are high, approximately 10^{-6} m s^{-1}, that is, about 100 m yr^{-1}. This is a spatially averaged estimate over tens to hundreds of meters and does not take into account finer-scale venting, which may be very heterogeneous. The results of this work may help estimate the quantity of metal elements transported through pore fluid migration at modern hydrothermal sites.

1. INTRODUCTION

Below the seafloor, especially in areas with submarine volcanic activities, such as at mid-ocean ridges and back-arc extension basins, there may be abundant mineral resources. Hydrothermal vents form due to intrusion of sub-seafloor volcanoes, where a variety of metal-rich hydrothermal fluids are vented from the seafloor, forming ore deposits as they travel (e.g., Rona 2003; Tsuji et al. 2012). The study of fluid migration patterns is of great importance in understanding large-scale metal sulfide deposition systems on the seafloor. Fluid activity also plays an important role in the mineralization systems during the circulation and interaction between magmas and surrounding rocks, which results in high alkalinity and high concentrations of CO_2 followed by phase separation processes (e.g., Glasby and Notsu 2003; Konno et al. 2006). However, it is difficult to conduct long-term and continuous direct observation of deep-sea and sub-seafloor hydrothermal activities using existing observation techniques. Therefore, numerical simulation in the field of computational geoscience offers an important alternative way to indirectly study these fluid migration systems.

The research area of this work is located at the southern tip of the Okinawa Trough (Fig. 1a). The Okinawa Trough is a back-arc spreading center in the rifting stage, generated as a result of the Philippine Sea Plate subducting beneath the Eurasian Plate (Lee et al. 1980; Letouzey and Kimura 1986; Sibuet et al. 1998). The northern boundary of the Okinawa Trough is adjacent to the shelf edge of the East China Sea, whereas the southern boundary joins the Ryukyu Island Arc. The spreading center extends southwestward to

* *Corresponding author*
E-mail: wchi@gate.sinica.edu.tw

northeastern Taiwan. Marine seismic refraction, in addition to gravity and other geophysical data indicate several north-south active extensional structures that may account for the thinned crust in this area (Sibuet et al. 1995). It is not clear whether the thermal fluid originates from crustal rifting, which causes pressure decrease and melting of the crust; or is generated by partial melting and dehydration that occurs during the subduction of the marine sediments.

The Okinawa Trough hosts many volcanic features and formations, including the Yonaguni Knoll IV (Fig. 1). To date, many volcanic formations and features had been discovered at Yonaguni Knoll IV, Okinawa Trough (Fig. 1). The Tiger Chimney and Lion Chimney of the Yonaguni Knoll IV are black smoker vents. Inagaki et al. (2006) measured the vent fluid temperature to 323°C. The venting mechanism is thought to be driven by magmatic sources (Sakai et al. 1990), and the resulting buoyancy forces hot water (hydrothermal fluid) to migrate to the surface as hydrothermal vents. The vents often carry metal and sulfide materials, which are emitted into the sea along weak fractures (e.g., faults). For instance, Gena et al. (2013) reported the occurrence of unusual minerals such as Pt-Cu-Fe-bearing bismuthinite and Sn-bearing chalcopyrite formed in an active black smoker of the Tiger sulfide chimney area located 1370 m below the sea-level. In addition to thermal transfer, hydrothermal circulation facilitates a major chemical exchange between the circulating seawater and the ocean crust and plays an important role in regulating the chemistry of the oceans (e.g., Elderfield et al. 1993; Elderfield and Schultz 1996). If numerical modeling techniques can be used to study geothermal, magmatic, and other processes, it may be possible to analyze sulfide mineralization

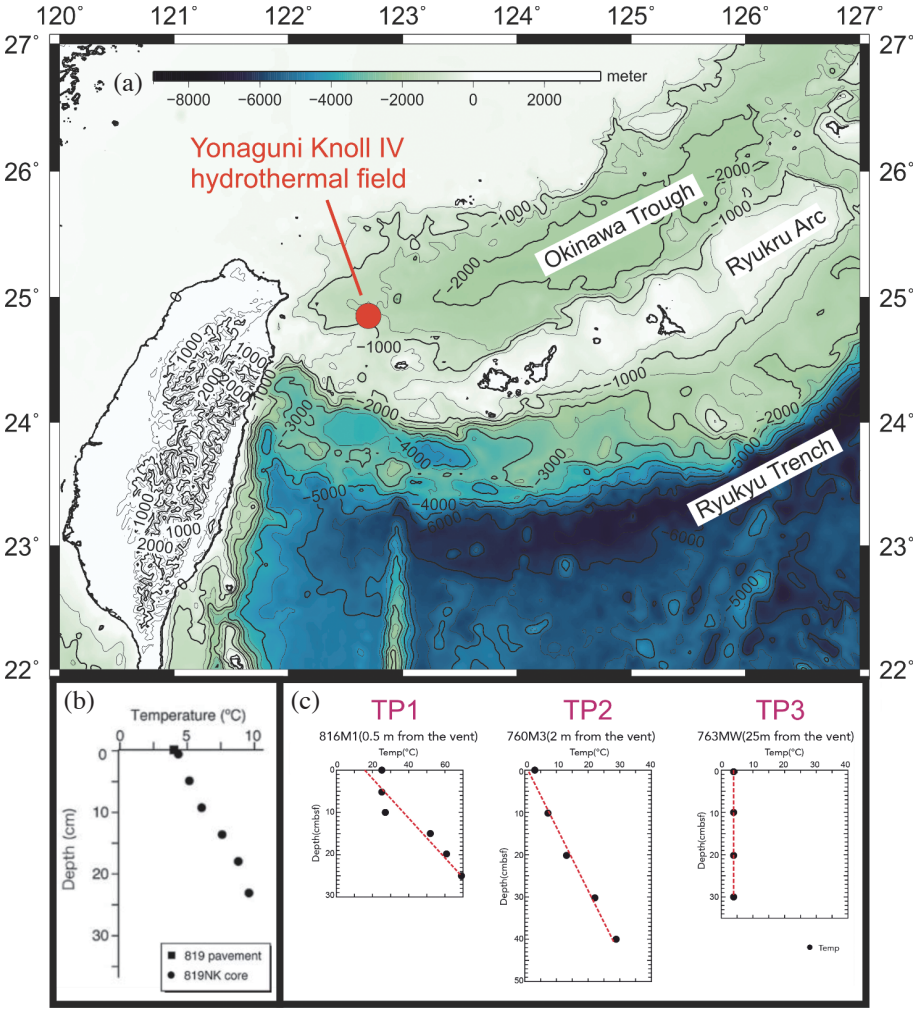

Fig. 1. Overview of the Yonaguni Knoll IV hydrothermal field and the temperature profile data used in this study. (a) Location map of the Yonaguni Knoll IV hydrothermal field in the southern Okinawa Trough. Grid data are obtained from the ETOPO1 Global Relief Model (Amante and Eakins 2009, freely available at https://www.ngdc.noaa.gov/mgg/global/). (b) Vertical profiles of temperature measured *in-situ*, from a supplementary figure in Inagaki et al. (2006). (c) *In-situ* temperature measurements of the sediment cores 816M1, 760M3, and 763MW at an abyss vent site, renamed Temperature Profiles (TP) 1, 2, and 3. Red dashed lines are linear regressions of the temperature profiles. Geothermal gradients obtained are approximately 2.1°C cm^{-1} at TP1, 0.7°C cm^{-1} at TP2, and close to 0°C cm^{-1} at TP3. Modified from Nunoura et al. (2010).

systems related to hydrogeology, which may advance our understanding of ore-forming mechanisms. However, modelling of large-scale polymetallic hydrothermal sulfide deposits can be extremely complicated, because hydrothermal fluids may exchange multiple times between deep magmatic sources and surrounding rock elements, resulting in the formation of hydrothermal minerals. It can also be a multiphase process including physical dissolution front (Zhao et al. 2010) and chemical dissolution front (Zhao et al. 2008a) instabilities. For this work, we do not consider chemical and phase changes, and only focus on shallow sub-seafloor deposits not in direct contact with magmatic sources. Nevertheless, the outcome of this work can further enrich the research contents of emerging computational geoscience, e.g., Zhao et al. (2009).

We use geophysical data such as *in-situ* temperature profiles and numerical simulation techniques to analyze the characteristics of hydrothermal activities. The fluid migration model is used to understand the thermal disturbance related to venting systems and to interpret theoretical heat flow patterns in space. Our model describes some key parameters that influence the potential of mineralization within the Okinawa Trough. Our goals are thus to: (1) Understand the physics behind heat conduction and convection. (2) Derive a first-order fluid flow rate estimate that explains *in-situ* temperature observations. (3) Discuss hydrothermal reformation and deposit patterns.

2. METHOD

We use two different methods to model fluid flux. The first is one-dimensional "Péclet number analysis" based on a single temperature profile with curvature, similar to Chen et al. (2012). The second method uses 3-D numerical modelling to derive fluid flow rate and direction based on known temperature profiles at different distances from a hydrothermal vent.

2.1 One-Dimensional Péclet Number Analysis and Fluid Flux Estimation of the Yonaguni Knoll IV

The temperature profile of a hydrothermal site in the Yonaguni Knoll IV (Fig. 1b) collected by Inagaki et al. (2006) is used to estimate the 1-D vertical fluid flux in this area. The *in-situ* temperature was collected with temperature probes on a push-core, at a site with leaking droplets of liquid CO_2, approximately 50 m southward from the Tiger and Lion chimneys (Inagaki et al. 2006). In this area, the temperature increased from 3.9°C in the overlying bottom water to 9.9°C at 35 cm sediment depth, indicating migration of hydrothermal fluids (Fig. 1b, Inagaki et al. 2006 published as supporting information on the PNAS website). For Péclet number analysis, we exclude data shallower than 10 cm because near-surface gradients likely experienced active mixing of bottom water and degassing during core recovery. Furthermore, visual inspection indicated a < 10 cm layer of solid ice-like CO_2 hydrates below the sediment cover (Inagaki et al. 2006), which is not appropriate to be simulated with calculation approaches for fluids with the possible heterogeneous permeability at the top 10 cm sediments.

The Péclet number (β) is a dimensionless value relevant to the study of transport phenomena in a continuum. In this study, it is defined to be the ratio of the rate of heat advection by the flow to the rate of heat conduction driven by an appropriate thermal gradient. When there is no groundwater flow, the thermal gradient is linear with depth, thus $\beta = 0$. As the groundwater velocity increases, β reflects the curvature on the thermal profile, concave upward or downward depending on the direction of the flow. Following Bredehoeft and Papaopulos (1965), we calculate β by fitting the curve of best fit with field thermal data, and then derive the 1-D fluid migration rate. The modelling procedure is as follows:

(1) Assume the seafloor is homogeneous and porous. The measured temperature data at different depths beneath the seafloor (T_z) are used as "actual observation data" for our simulation (Fig. 1b).

(2) Calculate the Péclet number (β) in the vertical direction at a steady state that corresponds to the local geothermal gradient from the 1-D model. We create a search grid with three variables, the temperature of the seafloor (T_0 with 1°C interval), the thickness of the porous layers (L with 1 cm interval), and the temperature of the bottom layer (T_L with 1°C interval), in order to find Péclet numbers at varying conditions. The formula is as follows:

$$\frac{T_z - T_0}{T_L - T_0} = \frac{e^{\beta z/L} - 1}{e^{\beta} - 1} \tag{1}$$

where T_0 = seafloor temperature (°C);
L = thickness of the homogeneous porous layer over which temperature measurements extend (m);
T_L = temperature at the bottom of the homogeneous porous layer (°C);
z = any depth below the seafloor (m);
T_z = temperature measurement at depth z below the seafloor (°C).

(3) Each condition in Step 2 corresponds to a single Péclet number. We choose the optimal Péclet number and the condition (T_0, L, T_L) which lead to the smallest temperature discrepancy (L2 norm) between the target value [left side of Eq. (1)] and the estimated value [right side of Eq. (1)], as shown in Eq. (2).

$$\text{Temperature discrepancy} = \sum_{z \in A} \frac{\left(\frac{e^{\beta z/L} - 1}{e^{\beta} - 1} - \frac{T_z - T_0}{T_L - T_0} \right)^2}{\left(\frac{T_z - T_0}{T_L - T_0} \right)^2} \tag{2}$$

where A is the set of depths of the observed data points (cm).

(4) This optimal Péclet number β is one of the key criteria needed for flow rate calculations, because it denotes the degree of bending that is caused by fluid velocity according to the local environmental conditions. We calculate the 1-D fluid velocity at which the fluid in the study area migrates in the porous layer using Eqs. (3) and (4).

$$\beta = \frac{\text{advective rate}}{\text{diffusive rate}} = \frac{\varepsilon \rho \gamma v L}{k} \tag{3}$$

$$v = \frac{\beta k}{\varepsilon \rho \gamma L} \tag{4}$$

where ε = rock's effective porosity (dimensionless);
ρ = fluid's density (kg m^{-3});
Υ = fluid's specific heat capacity (J kg^{-1} K^{-1});
v = fluid's velocity (m s^{-1});
L = thickness of the homogeneous porous layer (m);
k = rock's thermal conductivity (W m^{-1} K^{-1}).
Note that in this 1-D model, the fluid velocity is assumed to be constant throughout the homogenous porous layer. This is the main limitation of using the 1-D model.

2.2 Three-Dimensional Fluid Flux Estimation Based on a Cylindrical Vent Emission of the Yonaguni Knoll IV

We focus on the "abyss vent" site, which is characterized by 90°C hydrothermal emissions that discharge directly from the seafloor sediments (Nunoura et al. 2010). Sediment cores were taken at horizontal distances of 0.5, 2, and 5 m from the hydrothermal emission while simultaneously measuring the *in-situ* temperature of sediments (Fig. 1c, renamed as "Temperature Profiles" TP1, 2, and 3. Modified from Nunoura et al. 2010). Vertical geothermal gradients are estimated from the linear regressions to be 2.1°C cm^{-1} 0.5 m from the vent (TP1), 0.7°C cm^{-1} 2 m from the vent (TP2), and approximately 0°C cm^{-1} 5 m from the vent (TP3). The finite element commercial software COMSOL Multiphysics (version 5.3) is used to build a 3-D model (COMSOL Multiphysics® v. 5.3, COMSOL AB, Stockholm, Sweden, https://www.comsol.com).

2.2.1 Geometry, Mesh, and Physical Properties

First, a 2-D plane model is created with the geometry set to 1 meter deep, assuming a 15 cm pipe radius. Because it is axis-symmetric, the model is actually a 3-D cylinder with the mesh composed of tetrahedrons with side lengths of approximately 3 cm (Fig. 2).

Physical properties of each unit used in our model are listed in Fig. 2. All domains are set to be porous to allow the fluid to flow. We refer to the drilling data at the central Okinawa Trough (Takai et al. 2011) to assign a value of a porosity as high as 0.6 at the vent and 0.4 in the surrounding sediment. The thermal conductivity is derived from Chiao et al. (2016). For simplification, the fluid is assumed to be liquid-phase water and its dynamic viscosity is assumed to be 10^{-3} Pa·s. The vent is assumed to be highly permeable (permeability 10^{-12} m^2), twice as permeable as the surrounding sediments.

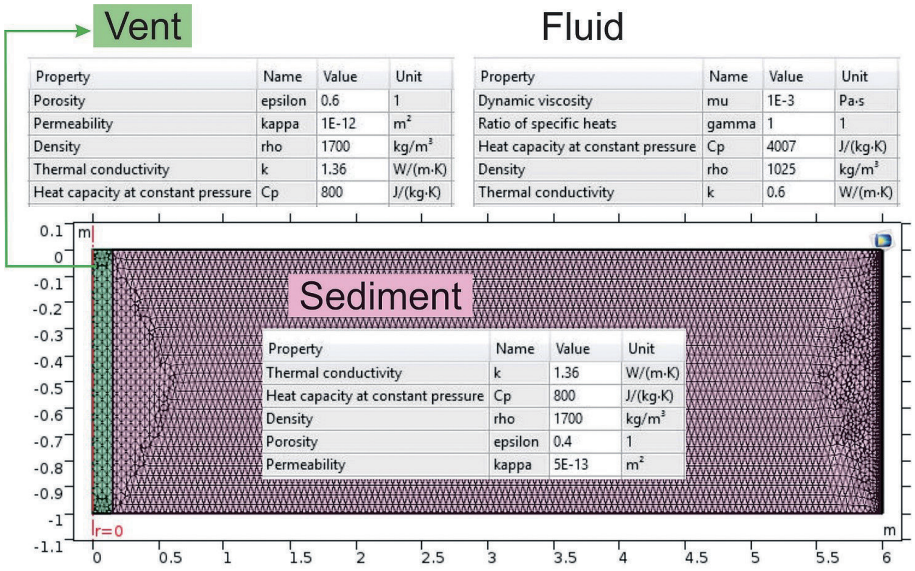

Property	Name	Value	Unit
Porosity	epsilon	0.6	1
Permeability	kappa	1E-12	m²
Density	rho	1700	kg/m³
Thermal conductivity	k	1.36	W/(m·K)
Heat capacity at constant pressure	Cp	800	J/(kg·K)

Property	Name	Value	Unit
Dynamic viscosity	mu	1E-3	Pa·s
Ratio of specific heats	gamma	1	1
Heat capacity at constant pressure	Cp	4007	J/(kg·K)
Density	rho	1025	kg/m³
Thermal conductivity	k	0.6	W/(m·K)

Property	Name	Value	Unit
Thermal conductivity	k	1.36	W/(m·K)
Heat capacity at constant pressure	Cp	800	J/(kg·K)
Density	rho	1700	kg/m³
Porosity	epsilon	0.4	1
Permeability	kappa	5E-13	m²

Fig. 2. Mesh and physical parameters of a 2-D slice of an axis-symmetric model. A vertical hydrothermal vent lies at the origin of the horizontal axis. Z-axis values denote the depth below the seafloor. Thermal conductivity is from Chiao et al. (2016). All the other parameters for the sediments and for fluid are typical as used in many numerical works.

2.2.2 Physics and Numerical Implementation

To combine thermal effects within both solid and fluid, the software's module "Heat Transfer in Porous Media" is used for heat flow calculations.

The module "Brinkman Equations" is used to calculate the fluid speed and pressure field of the subsurface flow. These equations extend Darcy's law to describe the dissipation of kinetic energy by viscous shear, similar to the Navier-Stokes equations. The model solves the continuity equation and momentum equation with Darcy's velocity and pressure as dependent variables. The "Gravity" feature is enabled to model the flow field in the presence of gravity acceleration. The compressibility option is set to weakly compressible.

The "Non-Isothermal Flow" multiphysics is enabled to couple the effects of flow and temperature. The simulation is run to a steady-state solution when both temperature and velocity field stabilize.

2.2.3 Initial and Boundary Conditions

The initial temperature is set to be 3.8°C (Wang et al. 2014) at the seafloor (z-axis 0 m), heating up below the seafloor with a gradient of 30°C km^{-1}. The initial pressure is set to be 1 atmospheric pressure + hydrostatic pressure of 1.3 km sea water (Chiao et al. 2016) + lithospheric pressure at each depth level. The vent has an initial temperature of 90°C. All domains have zero initial velocity.

The seafloor is set to be an outlet of hot groundwater with pressure as its boundary condition. The bottom boundary of the model is an inflow boundary with adjustable fluid speeds. At the top of the model, temperature at the seafloor (z-axis 0 m) is fixed to correspond to the observed seafloor temperature (Fig. 1c), with 90°C at the outlet of the vent (Nunoura et al. 2010). The side boundary is a no-slip wall and is thermally insulated. To run the model, different inflow speeds are tested and adjusted until the simulated temperature profile fits the observed data as closely as possible.

3. RESULTS

3.1 One-Dimensional Fluid Flux Estimation of the Yonaguni Knoll IV Hydrothermal Field

Figure 3 demonstrates a grid search of the temperature discrepancy at seafloor temperatures of 2°C, with varying thicknesses of the homogeneous porous layer and temperatures at depth L. The colors indicate the temperature discrepancy [defined in Eq. (2)] calculated in each grid. Similar grids are tested at varying seafloor temperatures from 1 - 5°C, but are not presented here for conciseness.

The optimal model (temperature discrepancy as small as 0.00047°C) is shown as a red cross in Fig. 3. In this model, the seafloor temperature (T_0) is equal to 2°C, the thickness of the homogeneous porous layer (L) is 0.33 m, the temperature at depth L under the seafloor (T_L) is 11°C, and the degree of bending (Péclet number) β caused by the fluid velocity is -1.6. Figure 4 is a normalized representation showing how the thermal curve with β = -1.6 fits the observations. In this case, "normalized depth" means the actual depth divided by 0.33 m, and "normalized temperature" is the actual temperature minus 2°C and then divided by 9°C [see left side of Eq. (1)].

Based on the highest value of *in-situ* heat flow data measured by Chiao et al. (2016) in this area, we assume a rock thermal conductivity of 1.36 W m^{-1} K^{-1}. Based on

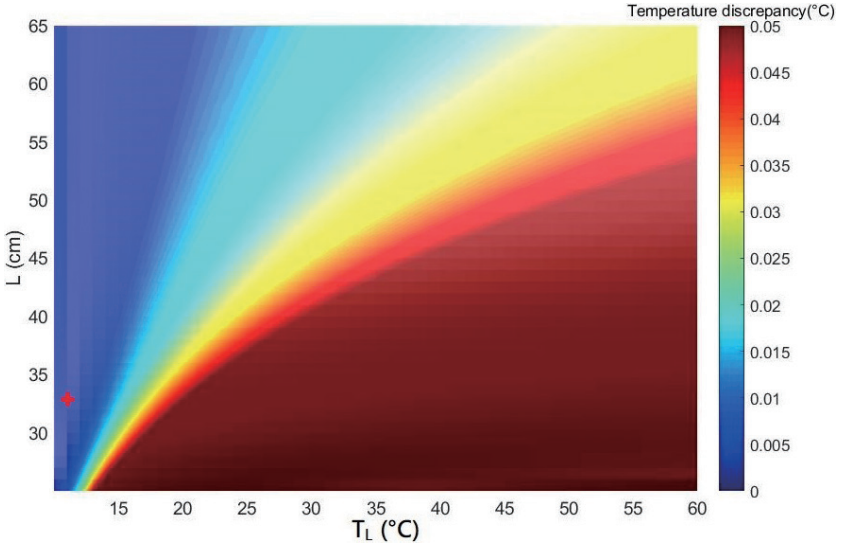

Fig. 3. Temperature discrepancy of the observed and estimated [defined in Eq. (2)] with a grid search at seafloor temperature T_0 = 2°C. L is the thickness of the homogeneous porous layer, and T_L is the temperature at the bottom of the homogeneous porous layer. The grid dimension is 50°C by 40 cm. The red cross marks the best solution with the smallest temperature discrepancy (0.00047°C), leading to L = 0.33 m and T_L = 11°C.

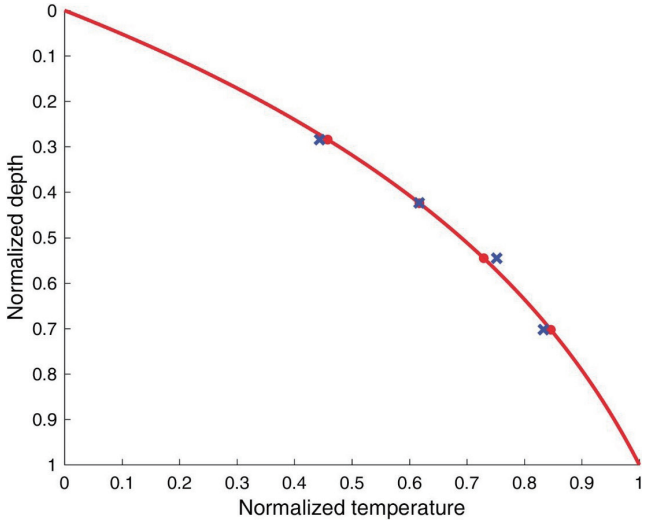

Fig. 4. Normalized representation of the actual temperature observations (blue crosses), versus the calculated temperatures based on the preferred model of the calculated Péclet number (red dots).

drilling data in the central Okinawa Trough by Takai et al. (2011), we set the effective porosity to 0.6. The fluid is assumed to have properties similar to those of seawater, with density 1025 kg m^{-3} and specific heat capacity 4007 J kg^{-1} K^{-1}. These values are substituted into Eq. (4) to estimate optimal fluid flow rate. The calculated result is v = (-1.6 × 1.36) / (0.6 × 1025 × 4007 × 0.33) ≈ -2.7 × 10^{-6} m s^{-1} ≈ -84 m yr^{-1}. The negative value indicates that the fluid is ejected from the sub-seafloor towards the surface of the seafloor, which is consistent with the visual seafloor observation of this site (Inagaki et al. 2006).

3.2 Three-Dimensional Fluid Flux Estimation of the Yonaguni Knoll IV Hydrothermal Field

The optimal model of the 3-D geothermal field is illustrated in Fig. 5a. A thermal plume is observed along the pipe because heat is carried upwards by the fluid. The dimensions of the plume are at least in part controlled by the surrounding fluid flow motion. Figure 5b shows a 2-D temperature profile (the origin of the abscissa is the center of this axial symmetric system), which is obtained from comparison with the observed data in Fig. 1c (TP1, 2, and 3). Observed data are pink, and simulated data are orange. The simulated data at 2 and 5 m distances from the vent are generally consistent with the observed data (TP2 and TP3), but the simulated geothermal gradient at the distance of 0.5 m is greater than the observed value (TP3). For a typical geothermal gradient of 30°C km^{-1}, a depth of 0.3 m translates to 0.009°C, thus the near-constant temperature profile 5 m from the vent (TP3).

The modelled fluid velocity field is shown in Fig. 5c. The color bar represents the velocity magnitude, and red arrows and white streamlines show the flow patterns. This figure is consistent with the interpretation that thermal water can either migrate along the pipe or leak through adjacent permeable domains. From this model, the calculated fluid velocity at the exit of the hydrothermal vent is about 3.7 × 10^{-6} m s^{-1} (≈117 m yr^{-1}), which is similar to the one-dimensional simulation discussed in the previous section. Based on the model assumption that the fissure diameter is 30 cm and the fluid density is 1.025 g cm^{-3}, the hydrothermal fluid flux emitted at this site is estimated to be about 2.7 × 10^{-4} kg s^{-1}, or 0.27 g s^{-1}.

4. DISCUSSION

4.1 One-Dimensional Modelling of the Yonaguni Knoll IV Hydrothermal Field

In the past, Bredehoeft and Papaopulos (1965) developed an analytical solution to describe vertical groundwater flow and suggested a type-curve method for estimating groundwater velocities from temperature data. In this work, we improve upon past approaches by using a grid search method, varying three parameters to get the preferred solution. From our preferred solution, which has a seafloor temperature (T_0) of 2°C, a homogeneous porous layer thickness (L) of 0.33 m, and a temperature at depth L (T_L) of 11°C, we can derive that the local geothermal gradient is approximately 27°C m^{-1} at the hydrothermal site. Because the temperature of hydrothermal fluids in the Yonaguni Knoll can be as high as 323°C (Inagaki et al. 2006), it can be speculated from our result that the latest stage heat source may be very shallow, a bit more than ten meters below the seafloor.

4.2 Three-Dimensional Modelling of the Yonaguni Knoll IV Hydrothermal Field

The numerical model does not provide a fluid flow rate

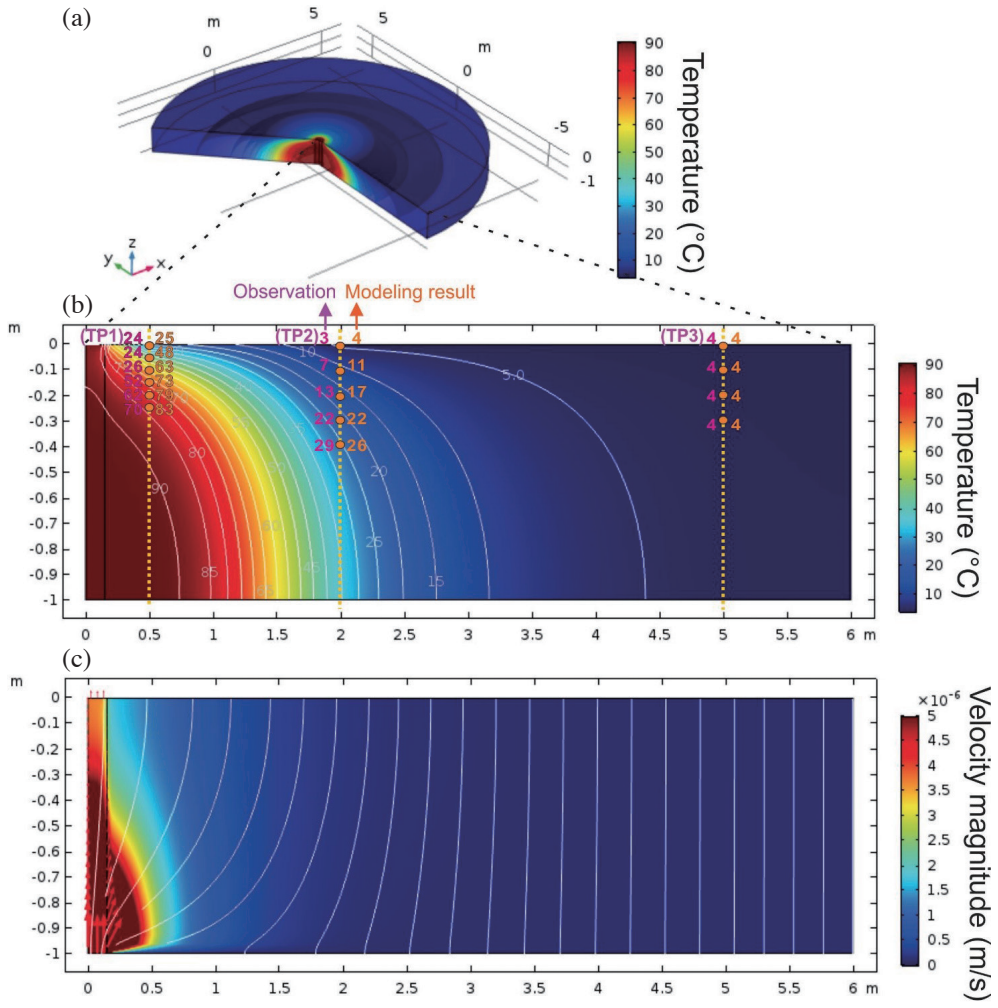

Fig. 5. Steady-state modelling result. TP1, 2, and 3 are the published data from Nunoura et al. (2010), see also Fig. 1c. (a) 3-D temperature representation. (b) 2-D temperature slice of 3-D numerical modelling. Thermal plume is observed due to hot fluid migration along the vent. Pink numbers denote the observed temperature (TP1, 2, and 3), and orange numbers represent the temperature simulated by the model. All values are rounded to whole digits. Coordinate units are in meters (twice vertical exaggeration). (c) 2-D profile of the fluid velocity field modelling result at steady state. Fluid migrates upwards along the vent, and into surrounding rocks. White lines are streamlines, and red arrows show direction. Modelling result shows that the velocity at the exit of the vent is approximately 3.7×10^{-6} m s^{-1}. Coordinate units are in meters (twice vertical exaggeration).

identical to the analytical model, but the results are on the same order of magnitude. The 1-D result should give only a first-order estimate, because the simulation assumes upward migration of fluid without considering the complex lateral changes in heat transfer patterns, even near the pipe, as seen in Fig. 5. The result from the 3-D simulation increases confidence in the models because it is consistent with the 1-D solution. The calculated fluid speeds can be compared with the regional vertical fluid migration rates offshore southwestern Taiwan, derived using bottom-simulating reflectors (Chen et al. 2012). Calculated values of between 84 and 117 m yr^{-1} correspond to 190 - 1950 times the known 1-D fluid migration rates from southwestern offshore Taiwan of between 6 and 44 cm yr^{-1} (Chen et al. 2012). These results are indicative of extensive hydrothermal activity in the Yonaguni Knoll IV. The estimated velocity is an average, as the system may be heterogeneous. For example, small gas bubbles may rise much faster than the surrounding water.

The 3-D simulation is an underdetermined system; there are not enough constraints to find a unique solution. The result of the numerical simulation is a possible solution based on assumed parameters. More data, such as geothermal probe data, core physical properties analysis, and high-resolution sonar images, may improve our existing model and result in a more reliable fluid flux estimation. Still, for the first time, the use of geophysical data provides an estimate of the fluid flux for this site.

4.3 Possible Parameters and Variations That Influence Hydrothermal Fluid Flow Patterns

To simplify our models, we assume the pore fluid

properties are similar to those of seawater. However, the exact salinity is unknown. In general, the density of a liquid increases as the salinity increases. On the other hand, if the liquid contains CO_2, the density decreases. Previous research shows that in the central and southern Okinawa Trough, hydrates have high levels of CO_2, and the observed emitted bubbles have the same magma source as the 320°C dissolved gas from the nearby black chimneys (Sakai et al. 1990). The results of geochemical analyses show that hydrothermal fluids may undergo complex and even heterogeneous (solid-liquid) evolution and coexistence (Konno et al. 2006; Suzuki et al. 2008). Therefore, we cannot exclude the possibility that fluid composition and possible geochemical reaction at high temperatures (for example, clay mineral dehydration at 60 - 150°C) might play important roles.

To simplify our model, we assumed that the migrating fluid was only in the liquid state. However, if gas is also present, it would be expected to induce greater thermal expansion. Therefore, the fluid rate calculated from our model is likely an underestimate. If a semi-quantitative analytical method can be developed to calculate the bubble flux at a vent site, the gas phase can be incorporated into the simulation of the hydrothermal activities, and the results may be relevant to future geophysical and geochemical studies. In our model, viscosity was assumed to be constant, but viscosity changes can exert a substantial influence on conditions for the onset of free thermal convection (e.g., Zhao et al. 2006, 2008b). We suspect that convection would occur more easily in a case with temperature-dependent fluid viscosity.

The fluid from a hydrothermal vent system may be sourced from magma and sediments, or from external recharge of seawater, which enters the system through the seafloor. As seen in Fig. 5c, no fluid recharge from the seafloor is observed in our model. Neither do we observe a convection cell (a type of transport that is induced by buoyancy in the fluid caused by the variation in density with temperature or composition). If convection cells are present at this site, their dimensions may be greater than our model, and in that case, permeability and fluid density variation may play key roles in controlling buoyant force and thermal convection. We suspect that permeability may be a highly sensitive parameter, because higher permeability would lead to more vigorous convection. It had been shown from the modelling result of Theissen-Krah et al. (2011) on mid-oceanic ridges that small changes in permeability would lead to large differences in the predicted temperature structure. A key direction to improve our model would be using geotechnical approaches (e.g., consolidation tests) to estimate the *in-situ* permeability structure for the set-up of the model, if coring samples are available.

Our model is built based on an idealized and simplified geometry. However, vent temperatures may decrease with increasing vent width because of mixing with ambient cold seawater. Andersen et al. (2015) modelled hydrothermal systems along the Mid-Atlantic Ridge located at outcropping fault zones. They found that to obtain the observed high temperature venting at the tip of the fault, it requires an optimal relative transmissibility (fault width times permeability contrast) which is high enough to "capture" a rising hydrothermal plume but low enough to prevent extensive mixing with ambient cold fluids. They also showed an intrinsic relationship that the higher the permeability, the higher the mass flux, and the lower the vent temperature. Therefore, hydrothermal fluid migration patterns are complexly controlled by different parameters. Currently, additional seismic investigations are being performed to better identify the structural features of the basin. To comprehensively improve the modelling technique, we should consider geometric heterogeneities and phase/chemical changes of groundwater, as these factors all affect local convection patterns.

5. CONCLUSION

In this paper, we developed the capability to use temperature as a tracer to study fluid flow patterns, and derived a first order-of-magnitude estimation of the fluid migration rates emitting from the thermal vents in the southern Okinawa Trough, currently interpreted as a back-arc spreading center. Temperature-fluid coupled one-dimensional analysis and three-dimensional numerical modelling of porous sediments give a range of fluid migration rates of 84 and 117 m yr^{-1}. This result is an average and does not consider bubbling and other small-scale processes. The modelling approaches were established to explain the change of vertical thermal gradient and the spatial variation of observed temperature fields.

The investigation of hydro-geothermal flow helps us understand the distribution and formation mechanism of seafloor hydrothermal sulfide deposits. Our results provide first-order spatial constraints for assessing the scale of fluid migration patterns in the survey area, which may assist in developing a more complete understanding of mineralization mechanisms at hydrothermal vents in general, a topic with potential social and economic benefits.

Acknowledgements This research is partially supported by the Central Geological Survey of Taiwan, project "Geological Investigation of Mineral Resource Potential in the Offshore Area of Northeastern Taiwan: Seismic and Heat Flow Surveys". We thank all the colleagues involved in this project, particularly Professor Char-Shine Liu, who contributed to data collection, processing, and interpretation of datasets. We also express our thanks to the anonymous reviewers for their valuable comments that improved the manuscript. T.-W. Wu thanks the additional research support from the MARUM. Bathymetry map was plotted using the Generic Mapping Tools (GMT) software.

REFERENCES

Amante, C. and B. W. Eakins, 2009: ETOPO1 1 Arc-Minute Global Relief Model: Procedures, Data Sources and Analysis. NOAA Technical Memorandum NESDIS NGDC-24, National Geophysical Data Center, NOAA, Boulder, Colorado, 25 pp, doi: 10.7289/V5C8276M. [Link]

Andersen, C., L. Rüpke, J. Hasenclever, I. Grevemeyer, and S. Petersen, 2015: Fault geometry and permeability contrast control vent temperatures at the Logatchev 1 hydrothermal field, Mid-Atlantic Ridge. *Geology*, **43**, 51-54, doi: 10.1130/G36113.1. [Link]

Bredehoeft, J. D. and I. S. Papaopulos, 1965: Rates of vertical groundwater movement estimated from the Earth's thermal profile. *Water Resour. Res.*, **1**, 325-328, doi: 10.1029/WR001i002p00325. [Link]

Chen, L., W.-C. Chi, C.-S. Liu, C.-T. Shyu, Y. Wang, and C.-Y. Lu, 2012: Deriving regional vertical fluid migration rates offshore southwestern Taiwan using bottom-simulating reflectors. *Mar. Geophys. Res.*, **33**, 379-388, doi: 10.1007/s11001-012-9162-4. [Link]

Chiao, L.-Y., H.-T. Chiang, C.-H. Wu, and J.-N. Wu, 2016: Geological Investigation of Mineral Resource Potential in the Offshore Area of Northeastern Taiwan: Seismic and Heat Flow Surveys (1/4): Heat Flow Surveys. Central Geological Survey, report No. 105-12-B, Taipei, 47 pp. (in Chinese with English abstract)

Elderfield, H. and A. Schultz, 1996: Mid-Ocean Ridge Hydrothermal Fluxes and the Chemical Composition of the Ocean. *Annu. Rev. Earth Planet. Sci.*, **24**, 191-224, doi: 10.1146/annurev.earth.24.1.191. [Link]

Elderfield, H., M. J. Greaves, M. D. Rudnicki, and D. J. Hydes, 1993: Aluminum reactivity in hydrothermal plumes at the Mid-Atlantic Ridge. *J. Geophys. Res.*, **98**, 9667-9670, doi: 10.1029/92JB01415. [Link]

Gena, K., H. Chiba, K. Kase, K. Nakashima, and D. Ishiyama, 2013: The Tiger Sulfide Chimney, Yonaguni Knoll IV Hydrothermal Field, Southern Okinawa Trough, Japan: The First Reported Occurrence of Pt-Cu-Fe-Bearing Bismuthinite and Sn-Bearing Chalcopyrite in an Active Seafloor Hydrothermal System. *Resour. Geol.*, **63**, 360-370, doi: 10.1111/rge.12015. [Link]

Glasby, G. P. and K. Notsu, 2003: Submarine hydrothermal mineralization in the Okinawa Trough, SW of Japan: An overview. *Ore Geol. Rev.*, **23**, 299-339, doi: 10.1016/j.oregeorev.2003.07.001. [Link]

Inagaki, F., M. M. M. Kuypers, U. Tsunogai, J. Ishibashi, K. Nakamura, T. Treude, S. Ohkubo, M. Nakaseama, K. Gena, H. Chiba, H. Hirayama, T. Nunoura, K. Takai, B. B. Jorgensen, K. Horikoshi, and A. Boetius, 2006: Microbial community in a sediment-hosted CO_2 lake of the southern Okinawa Trough hydrothermal system. *Proc. Natl. Acad. Sci.*, **103**, 14164-14169, doi: 10.1073/pnas.0606083103. [Link]

Konno, U., U. Tsunogai, F. Nakagawa, M. Nakaseama, J. Ishibashi, T. Nunoura, and K. Nakamura, 2006: Liquid CO_2 venting on the seafloor: Yonaguni Knoll IV hydrothermal system, Okinawa Trough. *Geophys. Res. Lett.*, **33**, L16607, doi: 10.1029/2006GL026115. [Link]

Lee, C.-S., G. G. Shor, L. D. Bibee, R. S. Lu, and T. W. C. Hilde, 1980: Okinawa Trough: Origin of a back-arc basin. *Mar. Geol.*, **35**, 219-241, doi: 10.1016/0025-3227(80)90032-8. [Link]

Letouzey, J. and M. Kimura, 1986: The Okinawa Trough: Genesis of a back-arc basin developing along a continental margin. *Tectonophysics*, **125**, 209-230, doi: 10.1016/0040-1951(86)90015-6. [Link]

Nunoura, T., H. Oida, M. Nakaseama, A. Kosaka, S. B. Ohkubo, T. Kikuchi, H. Kazama, S. Hosoi-Tanabe, K. Nakamura, M. Kinoshita, H. Hirayama, F. Inagaki, U. Tsunogai, J. Ishibashi, and K. Takai, 2010: Archaeal Diversity and Distribution along Thermal and Geochemical Gradients in Hydrothermal Sediments at the Yonaguni Knoll IV Hydrothermal Field in the Southern Okinawa Trough. *Appl. Environ. Microbiol.*, **76**, 1198-1211, doi: 10.1128/AEM.00924-09. [Link]

Rona, P. A., 2003: GEOLOGY: Resources of the Sea Floor. *Science*, **299**, 673-674, doi: 10.1126/science.1080679. [Link]

Sakai, H., T. Gamo, E.-S. Kim, M. Tsutsumi, T. Tanaka, J. Ishibashi, H. Wakita, M. Yamano, and T. Oomori, 1990: Venting of Carbon Dioxide-Rich Fluid and Hydrate Formation in Mid-Okinawa Trough Backarc Basin. *Science*, **248**, 1093-1096, doi: 10.1126/science.248.4959.1093. [Link]

Sibuet, J.-C., S.-K. Hsu, C.-T. Shyu, and C.-S. Liu, 1995: Structural and Kinematic Evolutions of the Okinawa Trough Backarc Basin. In: Taylor, B. (Ed.), Backarc Basins: Tectonics and Magmatism, Springer, Boston, MA, 343-379, doi: 10.1007/978-1-4615-1843-3_9. [Link]

Sibuet, J.-C., B. Deffontaines, S.-K. Hsu, N. Thareau, J.-P. Le Formal, and C.-S. Liu, 1998: Okinawa trough backarc basin: Early tectonic and magmatic evolution. *J. Geophys. Res.*, **103**, 30245-30267, doi: 10.1029/98JB01823. [Link]

Suzuki, R., J.-I. Ishibashi, M. Nakaseama, U. Konno, U. Tsunogai, K. Gena, and H. Chiba, 2008: Diverse Range of Mineralization Induced by Phase Separation of Hydrothermal Fluid: Case Study of the Yonaguni Knoll IV Hydrothermal Field in the Okinawa Trough Back-Arc Basin. *Resour. Geol.*, **58**, 267-288, doi: 10.1111/j.1751-3928.2008.00061.x. [Link]

Takai, K., M. J. Mottl, S. H. Nielsen, and the Expedition 331 Scientists, 2011: Proceedings of the Integrated Ocean Drilling Program, Volume 331 Expedition Reports,

Deep Hot Biosphere, Integrated Ocean Drilling Program Management International, Inc., Tokyo.

Theissen-Krah, S., K. Iyer, L. H. Rüpke, and J. P. Morgan, 2011: Coupled mechanical and hydrothermal modeling of crustal accretion at intermediate to fast spreading ridges. *Earth Planet. Sci. Lett.*, **311**, 275-286, doi: 10.1016/j.epsl.2011.09.018. [Link]

Tsuji, T., K. Takai, H. Oiwane, Y. Nakamura, Y. Masaki, H. Kumagai, M. Kinoshita, F. Yamamoto, T. Okano, and S. Kuramoto, 2012: Hydrothermal fluid flow system around the Iheya North Knoll in the mid-Okinawa trough based on seismic reflection data. *J. Volcanol. Geotherm. Res.*, **213-214**, 41-50, doi: 10.1016/j.jvolgeores.2011.11.007. [Link]

Wang, P., Q. Li, and C.-F. Li, 2014: Geology of the China Seas, Vol. 6, Elsevier, 702 pp.

Zhao, C., B. E. Hobbs, A. Ord, M. Kühn, H. B. Mühlhaus, and S. Peng, 2006: Numerical simulation of double-diffusion driven convective flow and rock alteration in three-dimensional fluid-saturated geological fault zones. *Comput. Meth. Appl. Mech. Eng.*, **195**, 2816-2840, doi: 10.1016/j.cma.2005.07.008. [Link]

Zhao, C., B. E. Hobbs, P. Hornby, A. Ord, S. Peng, and L. Liu, 2008a: Theoretical and numerical analyses of chemical-dissolution front instability in fluid-saturated porous rocks. *Int. J. Numer. Anal. Methods Geomech.*, **32**, 1107-1130, doi: 10.1002/nag.661. [Link]

Zhao, C., B. E. Hobbs, and A. Ord, 2008b: Convective Heat Transfer within Three-Dimensional Vertical Faults Heated from Below. In: Zhao, C., B. E. Hobbs, and A. Ord (Eds.), Convective and Advective Heat Transfer in Geological Systems, Advances in Geophysical and Environmental Mechanics and Mathematics, Springer, Berlin, Heidelberg, 145-159, doi: 10.1007/978-3-540-79511-7_9. [Link]

Zhao, C., B. E. Hobbs, and A. Ord, 2009: Fundamentals of Computational Geoscience: Numerical Methods and Algorithms, Springer-Verlag Berlin Heidelberg, Berlin, 323 pp, doi: 10.1007/978-3-540-89743-9. [Link]

Zhao, C., B. E. Hobbs, and A. Ord, 2010: Theoretical analyses of nonaqueous phase liquid dissolution-induced instability in two-dimensional fluid-saturated porous media. *Int. J. Numer. Anal. Methods Geomech.*, **34**, 1767-1796, doi: 10.1002/nag.880. [Link]